ELSEVIER

Thermochimica Acta 294 (1997) 173–178

thermochimica acta

Glass transition temperature and devitrification behaviour of lithium–titanium–germanate glasses

G. Laudisio, M. Catauro, A. Aronne, P. Pernice*

Department of Materials and Production Engineering, University "Federico II" Piazzale Tecchio, 80125 Napoli, Italy

Received 26 February 1996; accepted 12 December 1996

Abstract

The effect of replacing GeO_2 by TiO_2 on the glass-transition temperature and devitrification behaviour in lithium tetragermanate glass has been studied by differential thermal analysis, and Fourier- transform infrared spectra. The glass compositions are expressed by the general formula $Li_2OxTiO_2(4-x)GeO_2$ with $0.00 \leq x \leq 1.00$. The anion network of all glasses was found to contain GeO_4 and GeO_6 groups in the same molar ratio. The glass-transition and crystallisation temperature values are both increased by the progressive replacement of GeO_2 by TiO_2. Glasses with $x < 0.5$ devitrify into lithium tetragermanate crystals. Glasses with $x \geq 0.5$ devitrify in two steps into two non-identifiable phases. The influence on the crystallisation mechanisms of the specific surface of the samples was also pointed out. © 1997 Elsevier Science B.V.

1. Introduction

In previous papers [1–3] the non-isothermal devitrification of lithium tetragermanate, sodium tetragermanate and lead tetragermanate glasses has been investigated. The effect on the glass transition temperature and devitrification mechanism of the progressive replacing of Li_2O by Na_2O or PbO in binary germanate glasses were also pointed out [4,5].

$Li_2Ge_4O_9$, $Na_2Ge_4O_9$, and $PbGe_4O_9$ crystals have similar structures [6–8] formed by Ge_3O_9 rings, consisting of three GeO_4 tetrahedra, linked by GeO_6 octahedra giving a three-dimensional network. These structures can be characterised by the formulas $Li_2[Ge(GeO_3)_3]$, $Na_2[Ge(GeO_3)_3]$ and $Pb[Ge(GeO_3)_3]$. In spite of these similar structures, three different devitrification mechanisms were found. In lithium tetragermanate glass $Li_2Ge_4O_9$, microcrystallites are formed initially, and are then converted at higher temperatures into well-shaped $Li_2Ge_4O_9$ crystals [1]. Sodium tetragermanate glass crystallises in two steps. In the primary transformation, $Na_2Ge_4O_9$ crystals are formed that are then converted at higher temperatures into the thermodynamically stable $Na_4Ge_9O_{20}$ crystals [2]. Lead tetragermanate glass devitrifies in one step forming monoclinic and hexagonal $PbGe_4O_9$ crystals [3]. The progressive substitution of Na_2O for Li_2O causes the value of the glass-transition temperature to go through a deep minimum at molar ratio $Na_2O/Li_2O = 1$ in accordance with the 'mixed alkali effect' [4]. Replacement of Li_2O by PbO makes the network more tightly packed leading to a progressive increase in glass-transition temperature [5].

In the present work, the effect of a progressive replacement of GeO_2 by TiO_2 – that can behave as network former or network modifier – on the structure,

---

*Corresponding author. Fax: +39-81-7682595; e-mail: pernice@ds.cised.unina.it.

PII S0040-6031(97)00003-8

the glass-transition temperature and the devitrification behaviour of tetragermanate glasses were studied by differential thermal analysis (DTA) and Fourier-transform infrared spectroscopy (FTIR).

2. Experimental

The glass compositions are expressed by the general formula Li_2O $x TiO_2(4-x)GeO_2$, with $0.00 \leq x \leq 1.00$. In the course of the study, each glass is named by the corresponding x value. The glasses were prepared by mixing appropriate quantities of ultrapure lithium carbonate (Aldrich), titanium oxide (Aldrich) and germanium oxide (Heraeus) in a batch sized to yield 3 g of glass. The glasses were melted in an uncovered Pt crucible in an electric oven. The crucible containing the glass was weighed both before and after the glass was removed. The weight of the glass agreed with that anticipated from the batch calculation. This result indicates that the actual glass composition is close to that based on the glass batch. The melts were quenched by plunging the bottom of the crucible into cold water. Although this resulted in fracture of the glass, pieces of transparent glass of sizes sufficient for experimental measurements for all the compositions were obtained by this technique.

DTA curves were recorded in air at a heating rate of 10°C/min on bulk or fine powdered (<45 micron) specimens (~50 mg) from room temperature to 900°C. Powdered Al_2O_3 was added to improve heat transfer between bulk samples and sample holder. A Netzsch thermoanalyser high-temperature DSC 404 was used with Al_2O_3 as reference material. The experimental error in DTA temperature is ±1°C. The DTA curves have been elaborated by a Netzsch software.

Fourier-transform infrared (FTIR) absorption spectra were recorded in the 4000–400 cm^{-1} range using a Mattson 5020 system, equipped with a DTGS KBr (deuterated triglycine sulphate with potassium bromide windows) detector. A spectral resolution of 2 cm^{-1} was chosen. Each test sample was mixed with KBr (1 wt% of former) in an agate mortar, and then was pressed into 200 mg pellets of 13 mm diameter. The spectrum for each sample represents an average of 20 scans, which were normalised to the spectrum of the blank KBr pellet. The FTIR spectra have been analysed by a Mattson software (FIRST Macros). All the samples for IR measurements were heat-treated in a DTA furnace by quenching them directly after a DTA peak had occurred.

3. Results and discussion

Figs. 1 and 2 show the DTA curves of the as-quenched bulk glasses. A slope change occurs on all curves followed by one or more exothermic peaks. The slope change may be attributed to glass transition while the exothermic effects can be related to the heat evolved during the crystallisation processes.

When a glass is heated, its heat capacity – together with other properties – changes abruptly in a narrow temperature range, called the glass transition; this is

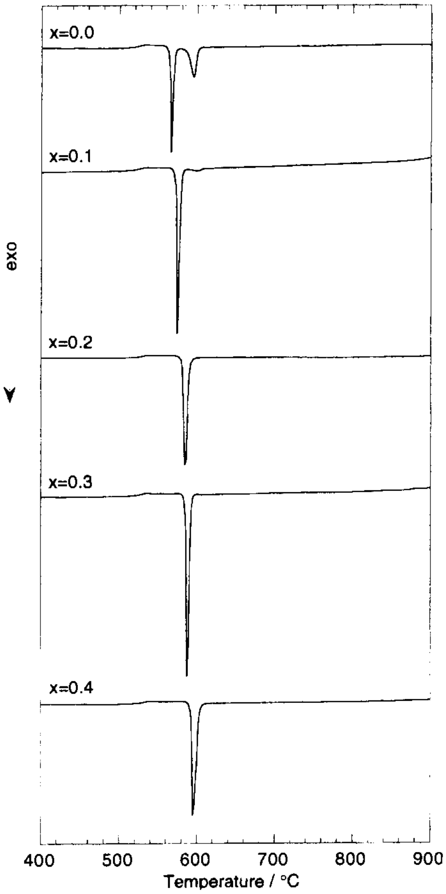

Fig. 1. DTA curves of the bulk glasses recorded at 10°C/min.

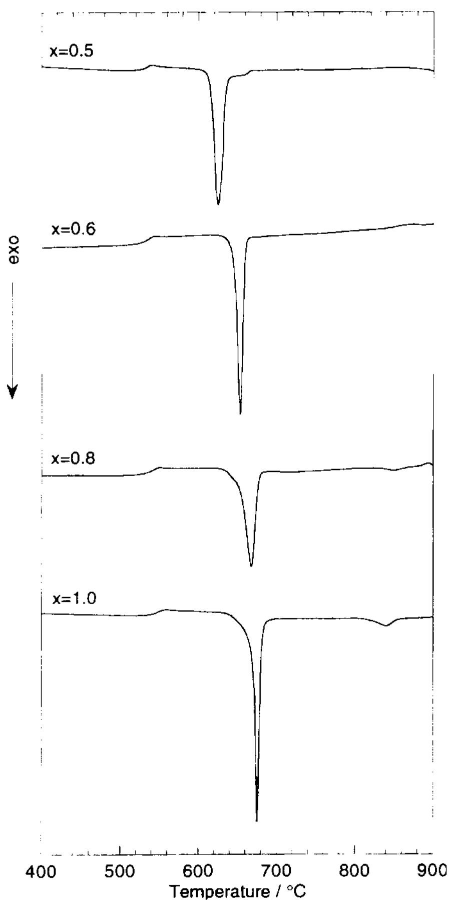

Fig. 2. DTA curves of the bulk glasses recorded at 10°C/min.

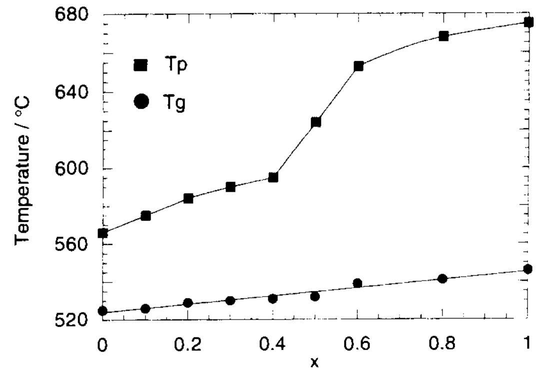

Fig. 3. Glass-transition temperature (T_g) and temperature of the first DTA exothermic peaks (T_p) as function of glass composition. Lines are used to connect the data points and are not curve fits.

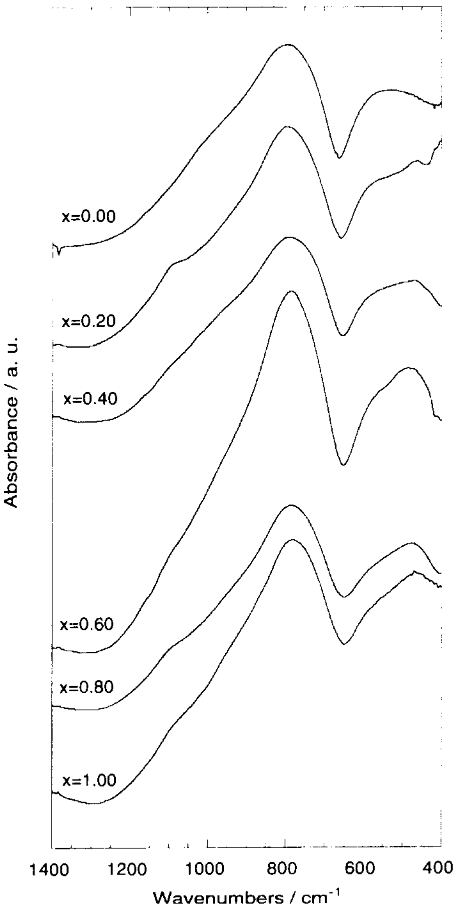

Fig. 4. FTIR absorption spectra of the studied glasses.

the transformation temperature range at which the glass network acquires mobility, changing from a rigid to a plastic structure. In this work, the inflection point at the slope change temperature of the DTA curve was taken as the glass-transition temperature, T_g. The reproducibility of T_g values is ±2 K. The values of T_g as well as the values of the temperature of the first DTA crystallisation peaks, T_p, for the investigated glasses are plotted as a function of x in Fig. 3.

The ionic radius of Ge^{4+} (0.53 Å) is very close to the cation/anion radius ratio limit that separates tetrahedral and octahedral co-ordination and, therefore, it can assume both fourfold and sixfold co-ordination. The FTIR absorbance spectra of the investigated glasses in the 400–1400 cm^{-1} range, where the Ge–O–Ge and O–Ge–O stretching and deformation modes are active, are shown in Fig. 4. These spectra exhibit broad bands as expected for glassy system. All glasses exhibit the highest absorption band at about 790 cm^{-1}. From previous studies [9], it is known that in the infrared spectra of hexagonal and vitreous GeO_2, in which the co-ordination number of germanium is 4, the absorption band at about 878 cm^{-1} is due to Ge–O–Ge stretching, while in tetragonal GeO_2, in which germanium assumes sixfold co-ordination, this band occurs at $\sim$688 cm^{-1}. In the absorption spectra of the investigated glasses, Fig. 4, the maximum of the absorption band due to Ge–O–Ge stretching shifts to lower wave numbers of about the same amount, 90 cm^{-1}, for each glass. This shift can be related, as in alkali–germanate glasses [10], to the change in the coordination number of Ge from 4 to 6. This interpretation according to the general notion that an increase in coordination number from XO_4 to XO_6 causes a decrease in X–O–X stretching frequency. These results indicate that the anion network of the studied glasses contains the same GeO_4/GeO_6 molar ratio. It was found that in lithium–titanium–silicate glasses Ti^{4+} ions are always in sixfold coordination and that the absorption band due to Ti–O–Ti symmetric stretching vibration occurs in the 661–695 cm^{-1} range [11]. The ionic size and the ionic charge of Ge^{4+} are very similar to that of Si^{4+} and, therefore, the chemistry of silicates and of the germanates resemble each other. The same behaviour should be, therefore, expected in lithium–titanium– germanate glasses. The observed trend in the T_g values can be related to the presence, in increasing number with x, of TiO_6 groups in the glass network. When GeO_2 is replaced by TiO_2, GeO_4 and GeO_6 groups have to be substituted by TiO_6 groups in equal amount so that the GeO_4/GeO_6 molar ratio can be keep unchanged. The increase of the total number of sixfold coordinated ions in the network leads to the increase in T_g values.

There are two types of crystallisation which take place in a glass, based on surface and bulk nucleations. The non-isothermal devitrification process is governed by the following equation [12].

$$-\ln(1-\alpha) = \frac{AN}{\beta^n}\exp\left(-\frac{nE}{RT}\right)$$

where α is the volume fraction crystallised at temperature T, E the activation energy of crystal growth, β the DTA heating rate and A a constant.

The number of nuclei, N, is the sum of surface nuclei proportional to the specific surface area of the samples and bulk nuclei formed during the heat treatments of the samples. The higher the number N, the lower is the temperature, T_p, of the DTA crystallisation peak [13].

The parameter n is related to the crystallisation mechanism. In the case of surface nucleation, nuclei are formed only on the surface and the crystals grow from the surface to the inside of the glass one-dimensionally ($n = 1$). In the case of bulk nucleation, each crystal particle grows three-dimensionally ($n = 3$). The shape of the crystallisation peak is strongly affected by the values of the parameter n, the higher the latter, the narrower the former [14], therefore surface and bulk crystallisations correspond to large and sharp peaks, respectively.

The shapes of the crystallisation peaks shown in Figs. 1 and 2 suggest a dominant bulk crystallisation in the glasses with $x \leq 0.4$, while in glasses with $x \geq 0.50$ surface crystallisation also occurs. To confirm these conclusions DTA curves on very fine-powdered samples were recorded. In Fig. 5 the gap between the temperature of the DTA crystallisation peak of bulk sample and that of the powdered sample is reported as a function of x. No appreciable shifts of the DTA peaks were detected on the DTA curves of the powdered glasses with $x < 0.5$, in which bulk crystallisation is dominant. In accordance with the great increase of number of surface nuclei due to the great increase of the specific surface area of the sample, the

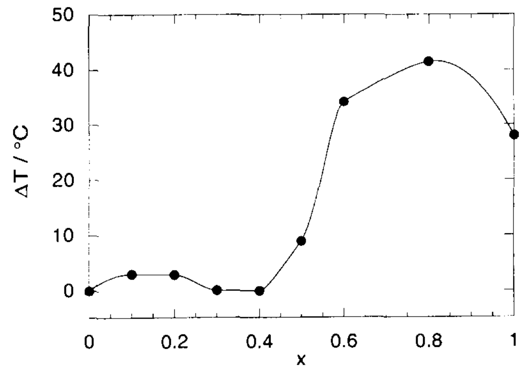

Fig. 5. Differences between crystallisation temperatures of bulk and powdered samples as function of glass composition. Line is used to connect the data points and does not represent curve fit.

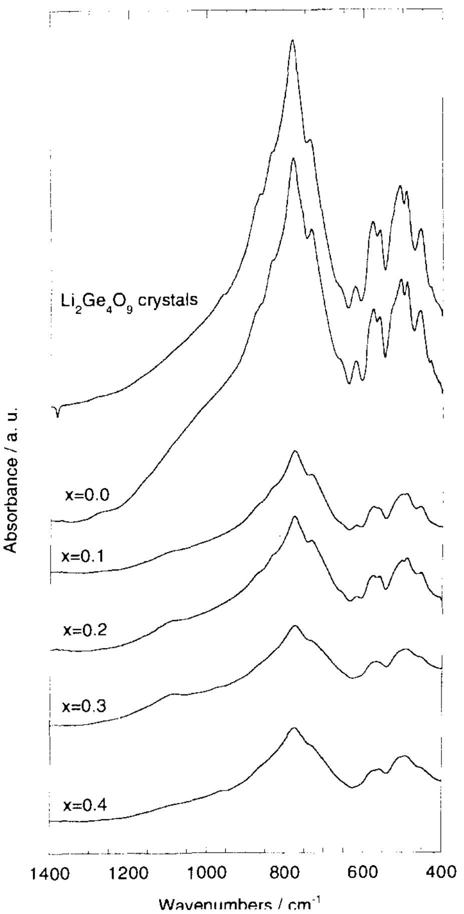

Fig. 6. FTIR absorption spectra of glasses with $x \leq 0.4$ heated up to the temperature of the first DTA crystallisation peak.

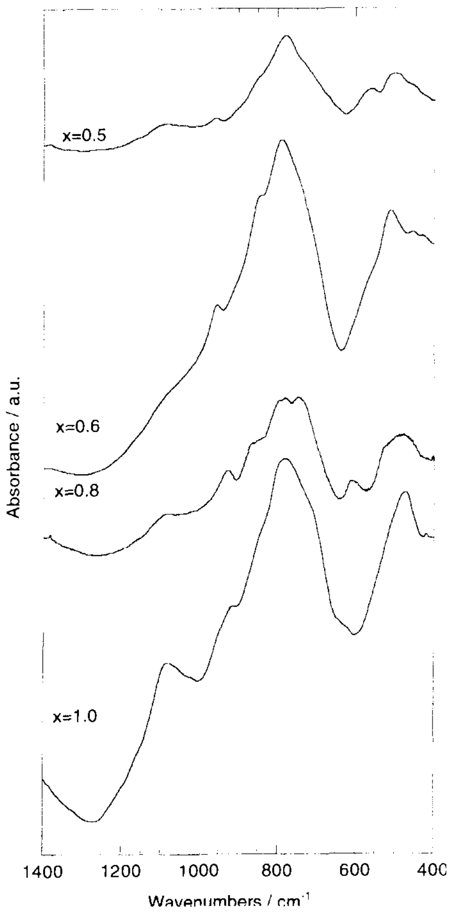

Fig. 7. FTIR absorption spectra of glasses with $x \geq 0.5$ heated up to the temperature of the first DTA crystallisation peak.

temperature of the DTA crystallisation peak of powdered glasses with $x \geq 0.5$, in which surface crystallisation takes place, is shifted towards lower temperatures.

Moreover on the DTA curves of the glass with $x \geq 0.5$, a second exothermic peak appears at ~800°C. Finally the gap between the crystallisation peak temperature, T_p, and the glass-transition temperature, T_g, is ~60°C in glasses with $x \leq 0.4$ and ~100°C in the other glasses.

The foregoing results suggest two different crystallisation mechanisms for glasses with $x < 0.5$ and for glasses with $x \geq 0.5$. To confirm this hypothesis the Fourier-transform infrared spectroscopy was used, as this technique is more sensitive than X-ray diffraction, to elucidate the initial stages of the crystallisation process: nucleation and crystal growth [15–17]. The FTIR spectra of the glasses heated to the temperature of each DTA crystallisation peak are reported in Figs. 6–8. It is noteworthy that the first exothermic peak on the DTA curve of the glass $x = 0.00$ does not lead to crystallisation but to a transformation in the glass [15]. The FTIR spectra of the glasses with $x \leq 0.4$, and of the stoichiometrically lithium tetragermanate crystals (Fig. 6), have similarities in position of the principal absorption bands, indicating that the same phase (lithium tetragermanate) crystallises in these glasses. The spectra of the glasses with $x \geq 0.5$ show that two new phases crystallise at the first Fig. 7 and second Fig. 8 exo-peaks. Further investigations have to be carried out to identify the nature of these phases.

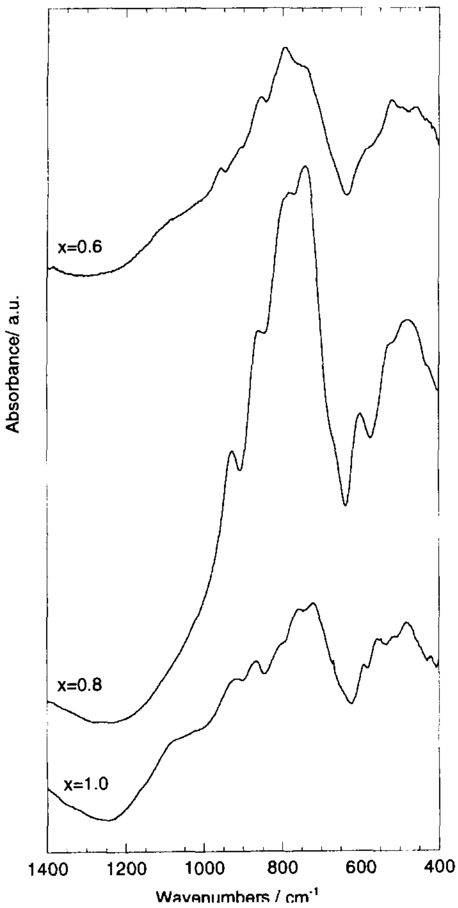

Fig. 8. FTIR absorption spectra of glasses with $x \geq 0.5$ heated up to the temperature of the second DTA crystallisation peak.

4. Conclusions

From the experimental results the following conclusions can be drawn:

1. The glass structures of all studied glasses contain the same GeO_4/GeO_6 molar ratio.
2. The replacement of GeO_2 by TiO_2 in the investigated glasses causes a progressive increase of the glass-transition temperature.
3. In glasses with $x \leq 0.4$ bulk crystallisation is dominant.
4. The devitrification processes of the investigated glasses occur in one or more steps. Glasses with $x \leq 0.4$ devitrify in a single stage into lithium tetragermanate crystals, whereas those with $x \geq 0.50$ devitrify, in two steps, into two unidentifiable crystalline phases.

References

[1] P. Pemice, A. Aronne and A. Marotta, Mater. Chem. Phys., 30 (1992) 195.
[2] A. Aronne, M. Catauro, P. Pemice and A. Marotta, Phys. Chem. Glasses, 35 (1994) 160.
[3] A. Aronne, M. Catauro and P. Pemice, Thermochim. Acta, 259 (1995) 269.
[4] A. MarottaA, A. Aronne, P. Pemice, and M. Catauro, Proceedings of the Second Conference of the European Society of Glass Science and Technology, Venice, Italy, 1993, Rivista Stazione Sperimentale del Vetro, Vol. 23 (1993) p. 430.
[5] A. Marotta, A. Aronne, P. Pemice and M. Catauro, Mater. Chem. Phys., 42 (1995) 247.
[6] A. Wittmann and E. Modem, Monatsh. Chem., 96 (1965) 581.
[7] K. Kamiya, T. Yoko, Y. Miki, Y. Itoh and S. Sakka, J. Non-Cryst. Solids, 91 (1987) 279.
[8] H.H. Otto and D. Dietrich, J. Appl. Crystallogr., 12 (1979) 421.
[9] J. Wong and C.A. Angell, in Glass Structure by Spectroscopy, Marcel Dekker, NY (1976) p. 456.
[10] M.K. Murthy and E.M. Kirby, Phys. Chem. Glasses, 5 (1964) 144.
[11] M.A. Villegas, A. de Pablos and J.M. Fernandez Navarro, J. Mater Sci., 30 (1995) 995.
[12] K. Matusita and S. Sakka, Bull. Inst. Chem. Res., Kyoto Univ., 59 (1981) 159.
[13] J.A. Augis and J.F. Bennet, J. Thermal. Anal., 13 (1978) 283.
[14] A. Marotta, A. Buri and F. Branda, J. Mater. Sci., 16 (1981) 341.
[15] A. Aronne, P. Pemice and M. Catauro, Phys. Chem. Glasses, in print.
[16] K.E. Lipinska-Kalita, J. Non-Cryst. Solids, 119 (1990) 41.
[17] S.K. Chen and H.S. Liu, J. Mater. Sci., 29 (1994) 2921.